Supporting Information

Morgan et al. 10.1073/pnas.1323681111

SI Text

Previously, a conditional HSD11B1 allele was generated by flanking exon 5 with LoxP sites (1). To generate adipose-specific 11β-hydroxysteroid dehydrogenase type 1 (11β-HSD1) KO mice (FKO), floxed homozygous HSD11B1 mice on a mixed C57 background were crossed with adiponectin-Cre transgenic mice (on a C57BL/6J background, targeting Cre expression to adipocytes). This generated mice devoid of 11β-HSD1 activity in adipose tissue. Genotyping PCR was carried out on ear-clip DNA using gene specific primers (5′-3′) P1-GGGAGCTTGCTTACAGCATC, P2-CATTCTCAAGGTAGATTGAACTCTG, and P3-TCCATGCAATCAACTTCTCG. P1+P2 give a 138-bp product for a WT allele and a 172-bp product for an allele containing a 3′ LoxP site. P1 and P3 give a 279-bp product for an allele after Cre recombination and exon 5 removal (Fig. S6*A*). Adipose tissues (gonadal, s.c., and brown) were the only tissues to show recombination, with other tissues (liver, muscle, lung, kidney, and heart) remaining normal for conditional HSD11B1 alleles (Fig. S6*B*). The 11β-HSD1 mRNA was reduced 0.16-fold, 0.17-fold, and 0.2-fold in gonadal, s.c., and brown adipose tissue of FKO mice, respectively; all other tissues studied had 11β-HSD1 mRNA similar to controls (Fig. S6*C*). The 11β-HSD1 oxo-reductase activity was reduced by 71% and 70% in s.c. and brown adipose tissue explants of FKO mice, respectively. Liver explants had activity similar to that of controls (Fig. S6*D*). Mature adipocytes extracted from gonadal, s.c., and brown adipose tissue of FKO mice had almost undetectable activity (<98% control activity), whereas the stromal vascular fraction extracted from these depots had activity similar to that of controls (Fig. S6*E*). Therefore, the 11β-HSD1 expressed in this subadipose tissue fraction is likely to explain the residual activity detected in the adipose tissue explants.

1. Semjonous NM, et al. (2011) Hexose-6-phosphate dehydrogenase contributes to skeletal muscle homeostasis independent of 11β-hydroxysteroid dehydrogenase type 1. *Endocrinology* 152(1):93–102.

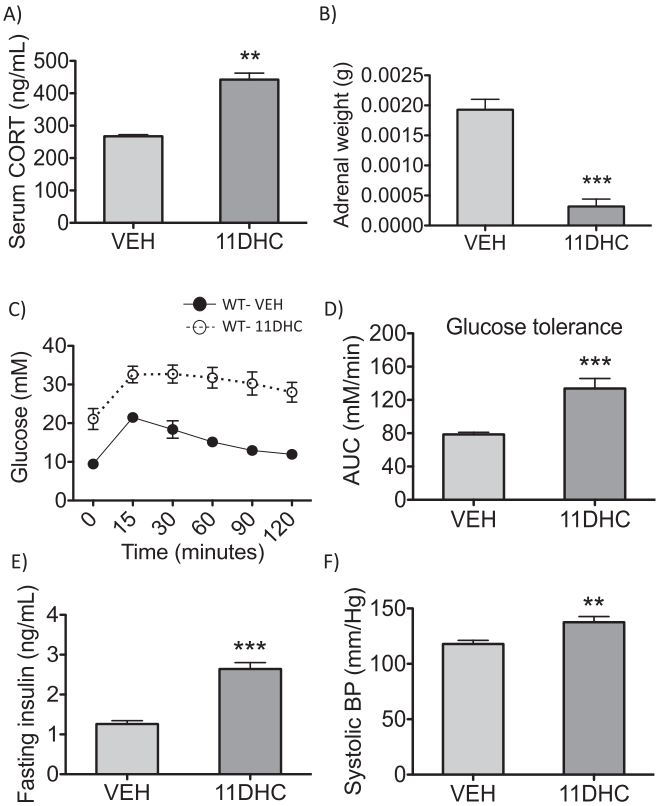

Fig. S1. Treatment with 11-dehydrocorticosterone (11DHC) induces glucose intolerance and hypertension in WT mice. C57BL/6 WT mice were treated with 11DHC (100 μg/mL) or vehicle via the drinking water for 5 wk (n = 7–9 in each group). Elevated circulating corticosterone (CORT) (*A*) and suppressed adrenal weights (*B*) were observed in 11DHC mice, and 11DHC induced glucose intolerance (*C* and *D*), increased fasting insulin levels (*E*), and increased systolic blood pressure (*F*) compared with vehicle-treated controls. Data were analyzed using two-way ANOVA; see Figs. 1 and 2 for the complete datasets used in the analysis. $^{**}P < 0.01$, $^{***}P < 0.001$ vs. WT vehicle.

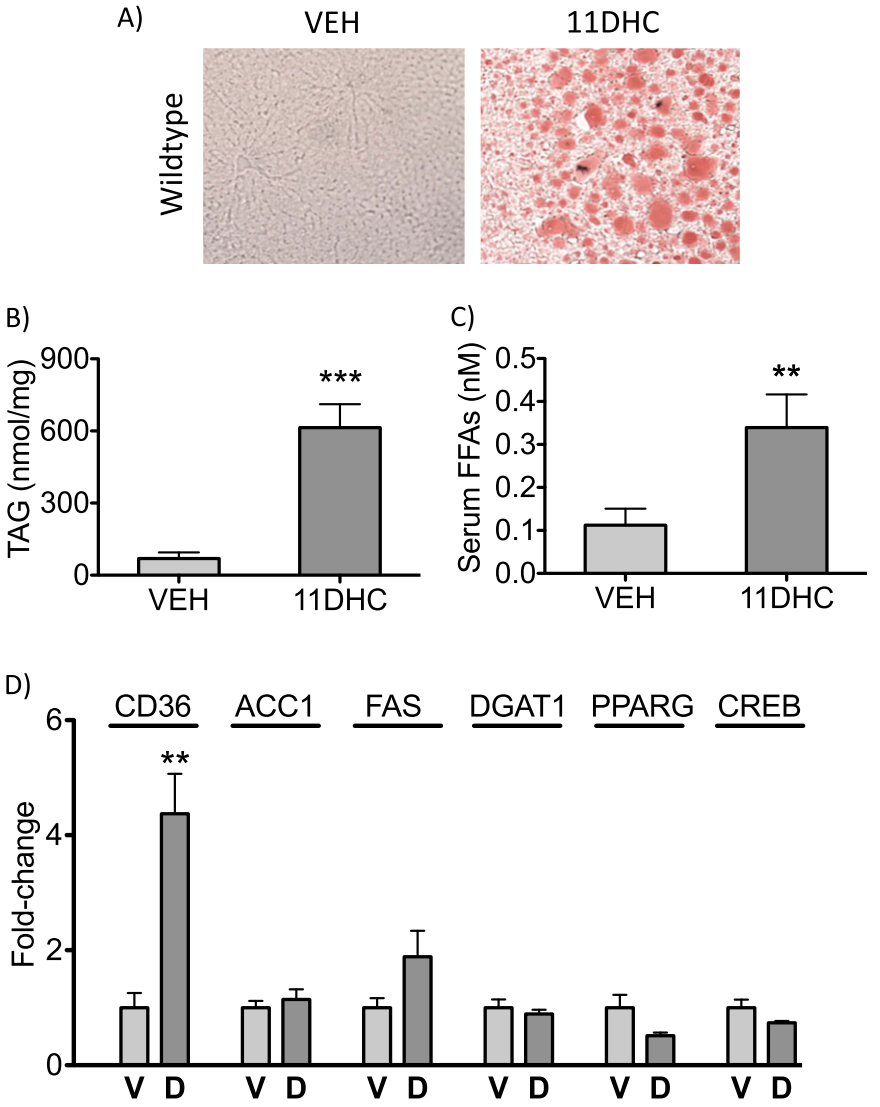

Fig. S2. Treatment with 11DHC induces hepatic steatosis in WT mice. Frozen liver sections stained with oil red O (*A*) and a quantitative triglyceride (TAG) assay (*B*) revealed increased hepatic TAG content of 11DHC-treated WT mice; 11DHC also increased serum free fatty acids (*C*) and increased hepatic mRNA expression of CD36 (*D*). The hepatic expression of the key lipogenic modulators acetyl-coA carboxylase 1 (ACC1), fatty acid synthase (FAS), diacylglycerol acyltransferase-1 (DGAT1), peroxisome proliferator-activated receptor-gamma (PPARG), and cAMP response element-binding protein (CREB) was unaffected by 11DHC treatment (*D*). Data were analyzed using two-way ANOVA; see Fig. 3 for the complete dataset used in the analysis ($n = 7–9$ in each group). $^{**}P < 0.01$, $^{***}P < 0.001$ vs. WT vehicle. D, 11DHC; V, vehicle,

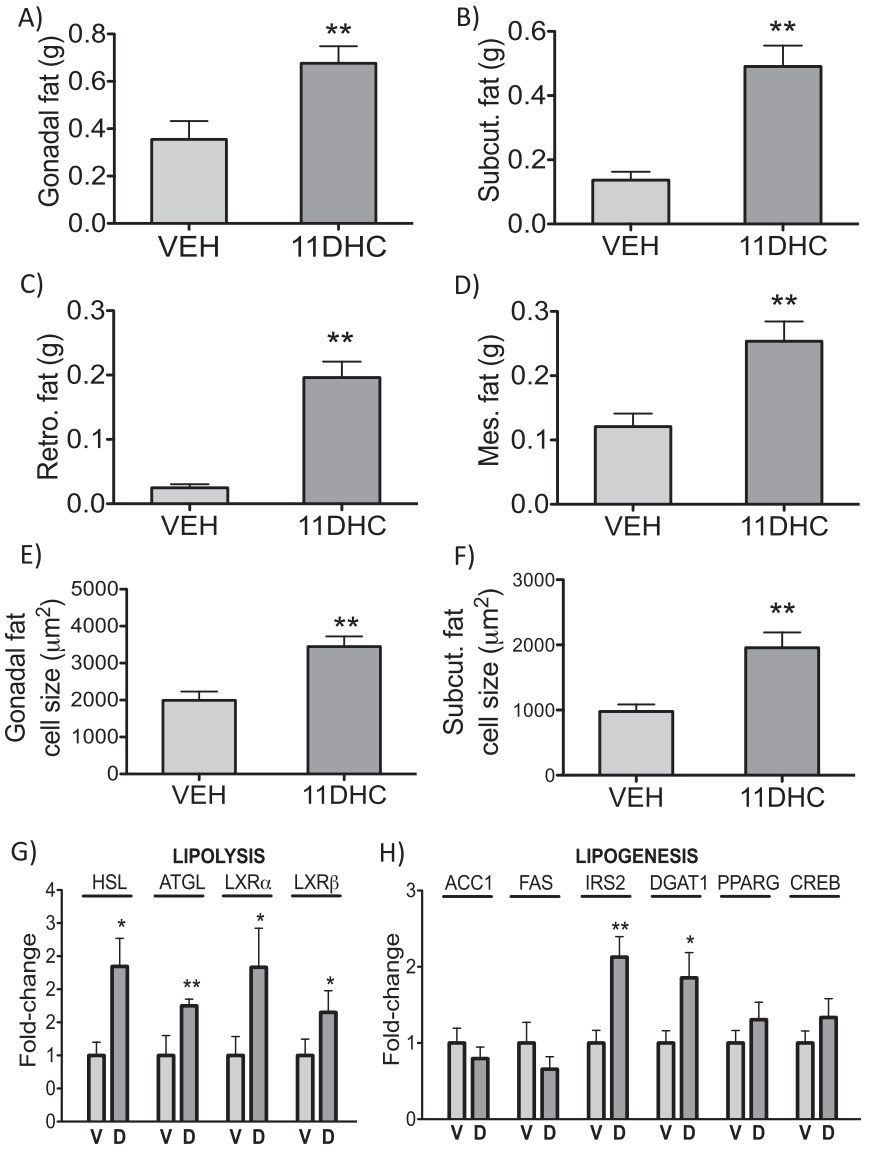

Fig. S3. Treatment with 11DHC increases adiposity in WT mice. The 11DHC treatment increased gonadal (*A*), s.c. (*B*), retroperitoneal (*C*), and mesenteric (*D*) adiposity in WT mice compared with vehicle-treated animals. H&E staining of paraffin-embedded gonadal and s.c. fat sections revealed increased adipocyte size in 11DHC-treated mice (*E* and *F*). The 11DHC increased the mRNA expression of key lipolytic genes in gonadal adipose tissue (*G*) ATGL, adipose triglyceride lipase; HSL, hormone-sensitive lipase; LXR, liver X receptor. The mRNA expression of the lipogenic mediators ACC1, FAS, PPARG, and CREB were unaffected by 11DHC treatment, whereas the expression of IRS2 and DGAT1 was increased (*H*). Data were analyzed using two-way ANOVA; see Fig. 4 for the complete dataset used in the analysis (n = 7–9 in each group). *$P < 0.05$, **$P < 0.01$ vs. WT vehicle. D, 11DHC; V, vehicle.

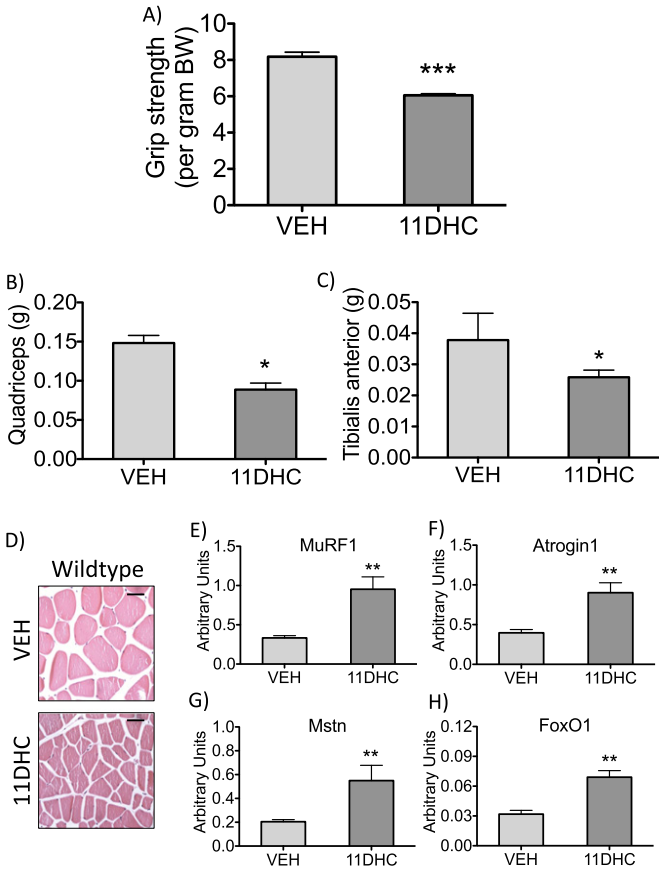

Fig. S4. Treatment with 11DHC induces myopathy in WT mice. Grip strength (*A*), quadriceps muscle bed weights (*B*), and tibialis anterior muscle bed weights (*C*) were reduced in 11DHC-treated WT mice. Paraffin-embedded quadriceps muscle sections stained with H&E revealed a smaller myofiber diameter in the 11DHC treatment group (*D*). (Scale bars, 200 μm.) Several muscle atrophy markers including muscle ring finger-1 (MuRF1) (*E*), atrogin-1 (*F*), myostatin (*G*), and forkhead box O1 (FoxO1) (*H*) were induced following 11DHC treatment. Data were analyzed using two-way ANOVA; see Fig. 5 for the complete dataset used in the analysis ($n = 7–9$ in each group). $^*P < 0.05$, $^{**}P < 0.01$, $^{***}P < 0.001$ vs. WT vehicle.

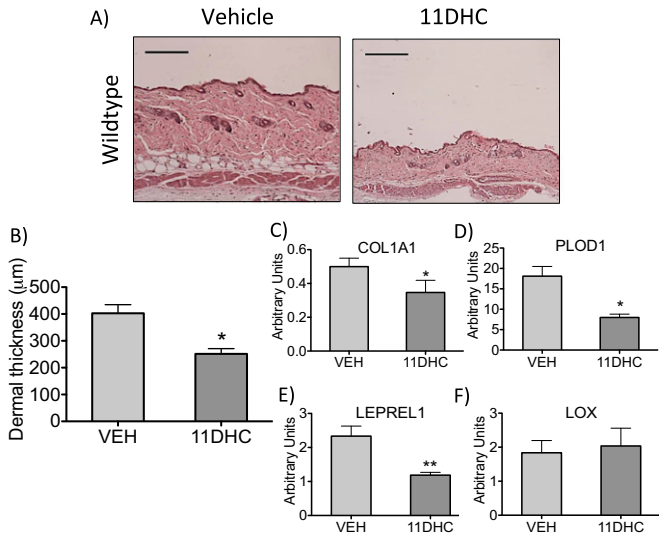

Fig. S5. Treatment with 11DHC induces skin thinning in WT mice. Paraffin-embedded skin sections stained with H&E revealed dramatically reduced skin thickness in WT mice following 11DHC treatment (*A*). (Scale bars, 200 μm.) Dermal thickness was quantified using ImageJ software (*B*). Several genes involved in collagen biosynthesis and processing in skin were induced by 11DHC, including Col1A1 (*C*), Leprel1 (*D*), and PLOD1 (*E*), but not LOX (*F*). ($n = 3$ in each group for skin histology and $n = 7–9$ in each group for gene expression). Data were analyzed using two-way ANOVA; see Fig. 6 for the complete dataset used in the analysis. $^*P < 0.05$, $^{**}P < 0.01$ vs. WT vehicle.

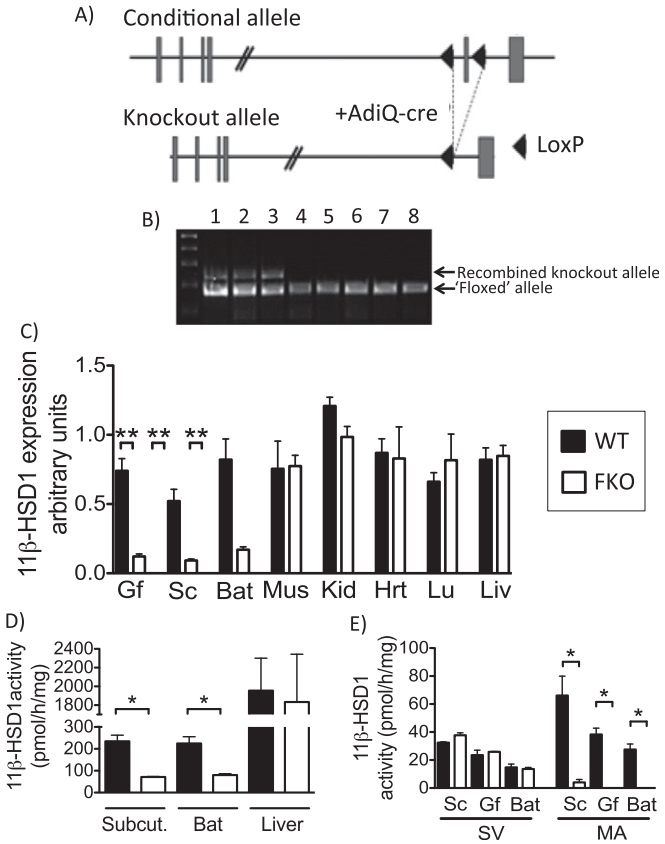

Fig. S6. Generation and validation of FKO mice. Targeting strategy for adipose-specific 11β-HSD1 KO mouse (FKO) generation (*A*). AdiQ-cre, adiponectin-cre. Genomic DNA PCR showing recombination is specific to adipose tissue, giving a null allele for 11β-HSD1 (*B*). Key for PCR: 1, brown fat; 2, s.c. fat; 3, gonadal fat; 4, heart; 5, kidney; 6, liver; 7, lung; and 8, muscle. mRNA levels of 11β-HSD1 in gonadal adipose tissue (Gf), s.c. adipose tissue (Sc), brown adipose tissue (Bat), skeletal muscle (Mus), kidney (Kid), heart (Hrt), lung (Lu), and liver (Liv) in control (white bars) vs. FKO mice (black bars) (*C*). The 11β-HSD1 oxo-reductase activity was significantly reduced in s.c. and brown adipose tissue explants of FKO mice. Liver explants had activity similar to that of controls (*D*). Mature adipocytes (MA) extracted from gonadal, s.c., and brown adipose tissue of FKO mice had almost undetectable activity, whereas the stromal vascular (SV) fraction extracted from these depots had activity similar to that of controls (*E*). $*P < 0.05$, $**P < 0.01$.

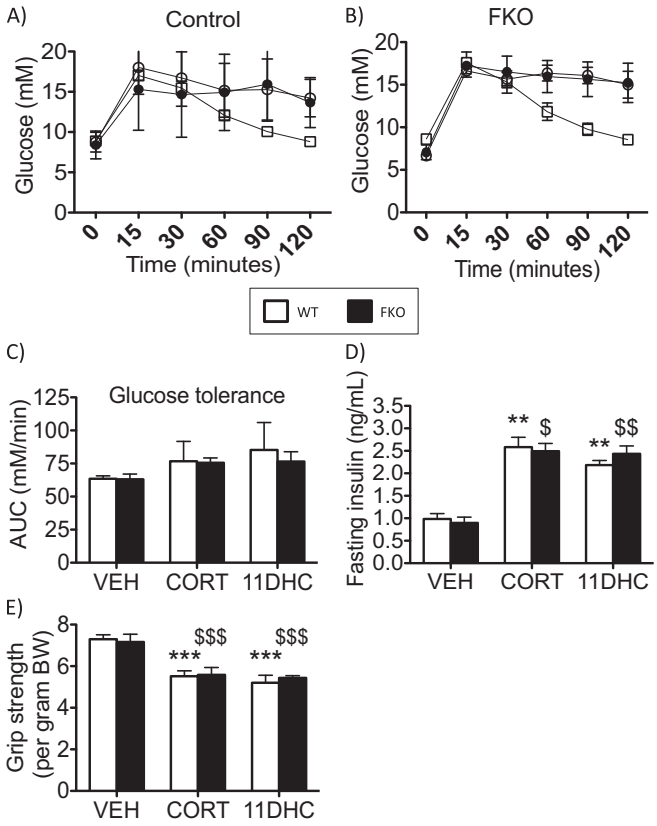

Fig. S7. FKO mice are not protected from the metabolic side effects induced by CORT or 11DHC. Both CORT and 11DHC treatment impaired glucose tolerance in control (*A*) and adipose-specific 11β-HSD1 KO (FKO) mice (*B*). □, vehicle; ●, 11DHC; ○, CORT. Calculated area under curves (AUC) for glucose tolerance data revealed no protection from glucose intolerance in FKO mice (black bars) compared with WT controls (white bars) following CORT and 11DHC treatment (*C*). Similarly, CORT and 11DHC elevated fasting insulin levels (*D*) and reduced grip strength (*E*) in both FKO and control mice, with the pattern of response being identical for the two genotypes. Data were analyzed using two-way ANOVA ($n = 6–7$ in each group). $^{**}P < 0.01$, $^{***}P < 0.001$ vs. WT vehicle; $^{\$}P < 0.05$, $^{\$\$}P < 0.01$, $^{\$\$\$}P < 0.001$ vs. KO vehicle. GTT: ⊟ VEH ⊸ 11DHC ⊖ CORT.

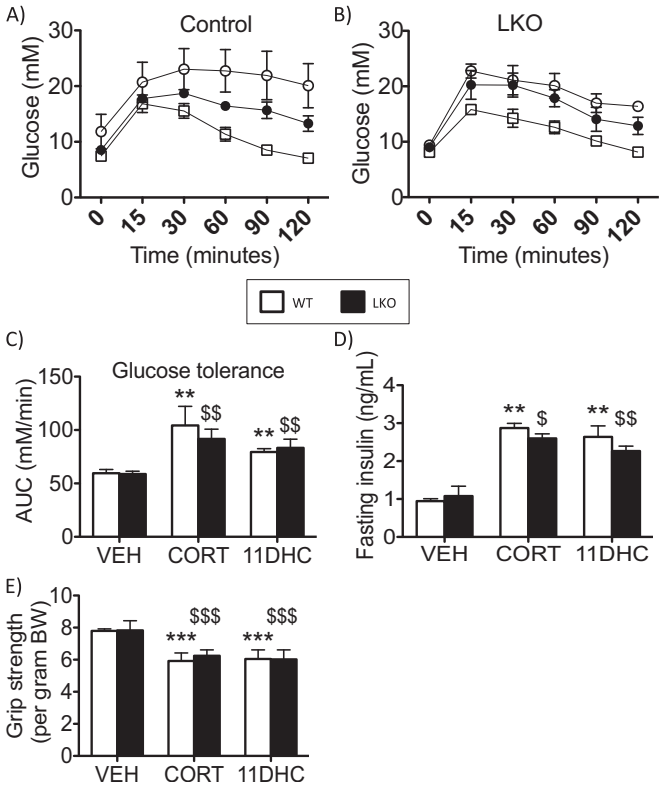

Fig. S8. LKO mice are not protected from the metabolic side effects induced by CORT or 11DHC. Both CORT and 11DHC impaired glucose tolerance in control (*A*) and liver-specific 11β-HSD1 KO mice (LKO) (*B*). □, vehicle; ●, 11DHC; ○, CORT. Calculated area under curves (AUC) for glucose tolerance data revealed no protection from glucose intolerance in LKO mice (black bars) compared with WT controls (white bars) following CORT and 11DHC treatment (*C*). Similarly, CORT and 11DHC elevated fasting insulin levels (*D*) and reduced grip strength (*E*) in both LKO and control mice, with the pattern of response being identical for the two genotypes. Data were analyzed using two-way ANOVA ($n = 6–7$ in each group). $^{**}P < 0.01$, $^{***}P < 0.001$ vs. WT vehicle; $^{\$\$}P < 0.01$, $^{\$\$\$}P < 0.001$ vs. KO vehicle. GTT: ⊟ VEH ⊸ 11DHC ⊖ CORT.

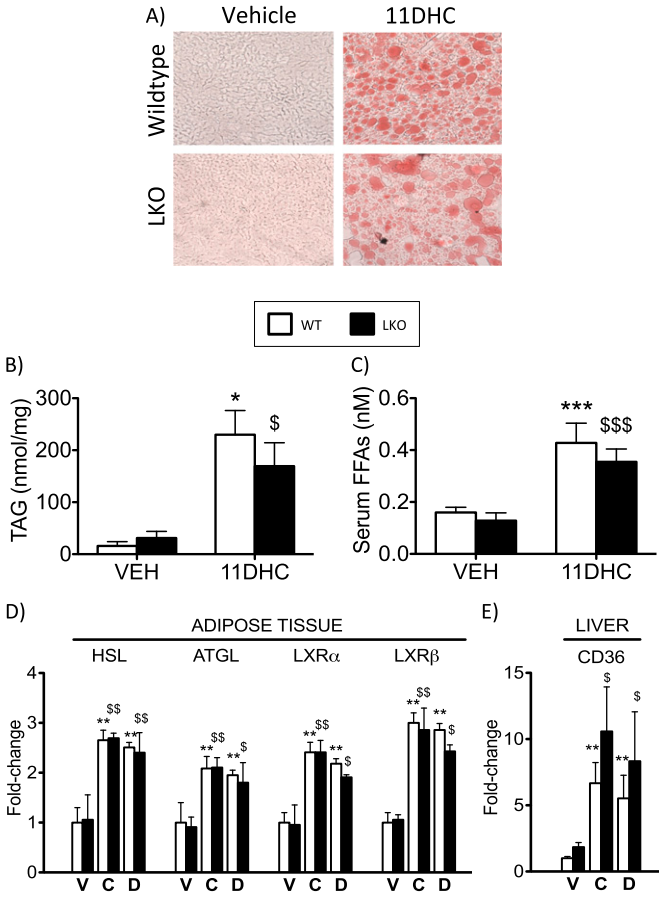

Fig. S9. LKO mice are not protected from the development of 11DHC-induced hepatic steatosis. Frozen liver sections stained with oil red O (*A*) and hepatic TAG quantification (*B*) revealed liver-specific 11β-HSD1 KO (LKO, black bars) mice are not protected from 11DHC-induced hepatic steartosis, compared with 11DHC-treated WT mice (white bars). Similarly, LKO mice were not shielded from increased serum free fatty acids (*C*), increased mRNA expression of lipolytic mediators in adipose tissue (*D*), or increased mRNA expression of the hepatic free fatty acid transporter CD36 (*E*) following 11DHC treatment. Data were analyzed using two-way ANOVA; see Fig. 7 for the complete dataset used in the analysis (n = 6–7 in each group). $^{*}P < 0.05$, $^{**}P < 0.01$, $^{***}P < 0.001$ vs. WT vehicle; $^{\$}P < 0.05$, $^{\$\$}P < 0.01$, $^{\$\$\$}P < 0.001$ vs. LKO vehicle. C, CORT; D, 11DHC; V, vehicle.

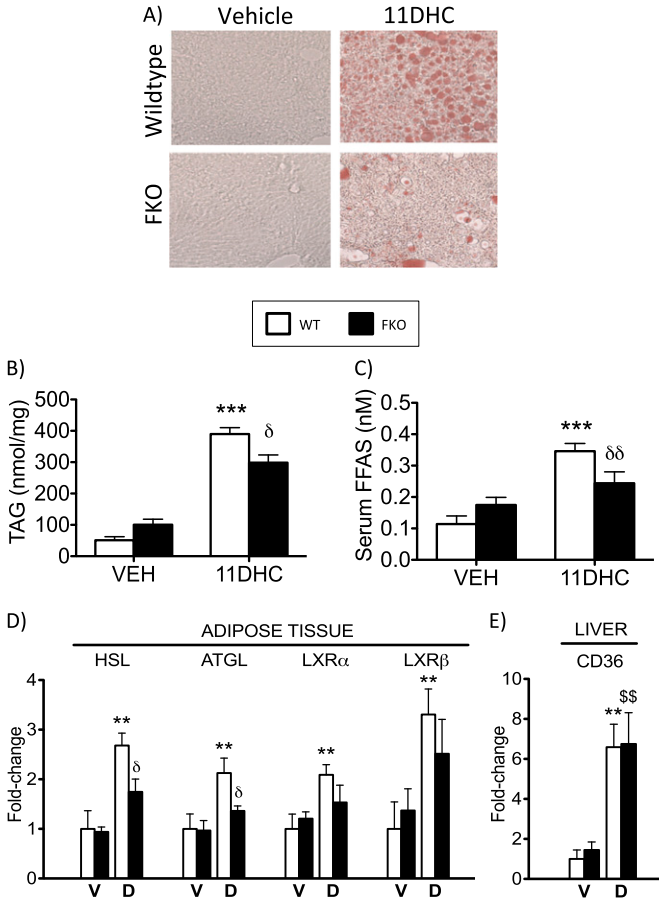

Fig. S10. FKO mice are protected from the development of 11DHC-induced hepatic steatosis. Frozen liver sections stained with oil red O (*A*) and a quantitative TAG assay (*B*) revealed fat-specific 11β-HSD1 KO (FKO, black bars) mice are protected from hepatic steatosis induced by 11DHC, compared with 11DHC-treated WT controls (white bars). Similarly, FKO mice were shielded from increased serum free fatty acids (*C*) and increased mRNA expression of lipolytic mediators in adipose tissue (*D*) following 11DHC treatment. FKO mice were not protected from increased expression of the hepatic free fatty acid transporter CD36 following 11DHC treatment (*E*). Data were analyzed using two-way ANOVA; see Fig. 7 for the complete dataset used in the analysis ($n = 6–7$ in each group). $^{**}P < 0.01$, $^{***}P < 0.001$ vs. WT vehicle; $^{\$\$}P < 0.01$ vs. FKO vehicle; $^{\delta}P < 0.05$, $^{\delta\delta}P < 0.01$ vs. WT 11DHC. D, 11DHC; V, vehicle.

Table S1. Tissue weights from liver-specific 11β-HSD1 KO (LKO) and control mice following treatment with CORT (100 μg/mL), 11DHC (100 μg/mL), or vehicle via drinking water for 5 wk

	Weight, mg ± SE					
	Control			LKO		
Tissues	Vehicle	CORT	11DHC	Vehicle	CORT	11DHC
Body weight, g	23.69 ± 1.88	22.90 ± 1.10	22.61 ± 0.89	24.50 ± 0.87	23.85 ± 1.24	24.13 ± 1.46
Quadriceps	152 ± 12	79 ± 15*	108 ± 2†	214 ± 49	131 ± 29§	127 ± 8§
Tibialis anterior	48 ± 3	31 ± 4†	38 ± 5	48 ± 3	39 ± 4	37 ± 2§
Soleus	6.8 ± 0.6	6.7 ± 1	5.7 ± 0.5	7.1 ± 0.2	5.1 ± 0.8	6.0 ± 0.3
Gonadal fat	264 ± 38	621 ± 98*	377 ± 68†	244 ± 13	442 ± 74§	373 ± 102§
Mesenteric fat	55 ± 10	321 ± 46‡	217 ± 35‡	53 ± 11	347 ± 34¶	363 ± 42¶
Retroperitoneal fat	73 ± 29	232 ± 47*	146 ± 35†	71 ± 11	165 ± 37$^{\|}$	166 ± 60§
Subcutaneous fat	245 ± 36	688 ± 104*	442 ± 43*	226 ± 31	528 ± 84$^{\|}$	371 ± 107§
Adrenal gland	1.4 ± 0.2	0.4 ± 0.1‡	0.4 ± 0.1‡	1.7 ± 0.1	0.4 ± 0.1¶	0.3 ± 0.1¶
Liver	1,088 ± 69	1,172 ± 67	1,055 ± 20	1,076 ± 77	1,182 ± 132	1,041 ± 52
Kidney	174 ± 10	153 ± 6	136 ± 6	167 ± 6	170 ± 8	169 ± 20

Data were analyzed using two-way ANOVA ($n = 6–7$ in each group). $^{\dagger}P < 0.05$, $^{*}P < 0.01$ $^{\ddagger}P < 0.001$ vs. WT vehicle; $^{\S}P < 0.05$, $^{\|}P < 0.01$, $^{\P}P < 0.01$ vs. LKO vehicle.

Table S2. Tissue weights from adipose-specific 11β-HSD1 KO mice (FKO) and control mice following treatment with CORT (100 μg/mL), 11DHC (100 μg/mL), or vehicle via drinking water for 5 wk

	Weight, mg ± SE					
	Control			FKO		
Tissues	Vehicle	CORT	11DHC	Vehicle	CORT	11DHC
Body weight, g	27.74 ± 0.53	29.69 ± 0.39	27.26 ± 1.42	27.75 ± 0.48	29.73 ± 0.55	29.44 ± 0.67
Quadriceps	170 ± 8	99 ± 12*	123 ± 5*	172 ± 11	116 ± 6‡	118 ± 14‡
Tibialis anterior	58 ± 0.0031	34 ± 2.9*	29 ± 3.3*	50 ± 1.6	32 ± 3.7‡	38 ± 5.6§
Soleus	7.9 ± 0.5	9.7 ± 1.2	6.1 ± 0.5	10.6 ± 1.6	5.8 ± 1.1	6.6 ± 0.3
Gonadal fat	345 ± 29	946 ± 114*	830 ± 26†	360 ± 21	802 ± 79‡	827 ± 84‡
Mesenteric fat	88 ± 24	240 ± 43	335 ± 88	68 ± 9	210 ± 13	269 ± 28
Retroperitoneal fat	86 ± 16	319 ± 45*	390 ± 50*	84 ± 10	306 ± 27‡	367 ± 21‡
Subcutaneous fat	230 ± 28	987 ± 58†	1111 ± 54†	186 ± 22	976 ± 77¶	913 ± 195‡
Adrenal gland	1.8 ± 0.1	0.7 ± 0.1†	0.6 ± 0.2†	1.6 ± 0.1	0.5 ± 0.1¶	0.5 ± 0.2¶
Liver	1,060 ± 40	1,648 ± 189	1,098 ± 67	1,107 ± 115	1,243 ± 58	1,072 ± 105
Kidney	170 ± 7	160 ± 8	153 ± 1	157 ± 5	175 ± 32	173 ± 9

Data were analyzed using two-way ANOVA ($n = 6–7$ in each group). *$P < 0.01$ $^{†}P < 0.001$ vs. WT vehicle; $^{§}P < 0.05$, $^{‡}P < 0.01$, $^{¶}P < 0.01$ vs. FKO vehicle.